ELSEVIER

Journal of Nuclear Materials 317 (2003) 109–116

journal of nuclear materials

www.elsevier.com/locate/jnucmat

Thermophysical studies on the binary system $UO_2(NO_3)_2 \cdot 6H_2O$ – $Sr(NO_3)_2$

P.V. Ravindran [a,*], B.B. Kalekar [a], K.V. Rajagopalan [a],
C.G.S. Pillai [b], P.K. Mathur [a]

[a] *Analytical Chemistry Division, Bhabha Atomic Research Centre, Trombay, Mumbai 400 085, India*
[b] *Novel Materials and Structural Chemistry Division, Bhabha Atomic Research Centre, Trombay, Mumbai 400 085, India*

Received 9 February 2001; accepted 7 January 2003

Abstract

Thermoanalytical (TG-DTA-EGA) and X-ray diffraction measurements have been used to study the reaction between uranyl nitrate hexahydrate and strontium nitrate. The results confirmed the absence of a direct interaction between the two compounds. The presence of strontium nitrate, however, ensured that the extent of hydrolysis and polymerisation of uranyl nitrate hexahydrate during its dehydration and decomposition to UO_3 is significantly reduced. DTA curves recorded in both heating and cooling modes gave evidence to the occurrence of a reaction between molten strontium nitrate and uranium trioxide to form nitrato-complexes of uranium and strontium. X-ray diffraction data on reaction residues obtained at different temperatures and cooled to room temperature also showed evidence for the formation of such complexes. The results obtained indicated an increase in thermal stability of these nitrato-complexes with increase in Sr/U ratio. The complex with an Sr/U ratio of 2.0 is stable up to 660 °C and the complex with Sr/U ratio of 4.0 is stable up to 680 °C. These complexes decompose at higher temperatures to give strontium uranates.

---

1. Introduction

High-temperature interactions in the multiphase system involving actinide nitrates, alkali and alkaline-earth metal nitrates, rare-earth nitrates, nitrates of chromium, iron, nickel, cobalt, zirconium and aluminium are of interest from the point of view of optimising the conditions for calcination and incorporation of the resulting oxides in glass matrix. In an earlier study, Mukerji and Kanyal [1] reported the reaction of individual nitrates of the alkali and alkaline-earth metals with glass forming additives, like, silica, alumina and metakaolinite. However, the possibility of mixtures of the nitrates forming intermediate nitrato-complexes, which decompose to form mixed oxides has been demonstrated in a recent work [2] carried out in our laboratory. We obtained evidence for the formation of new intermediate nitrates, which decomposed to form sodium diuranate, in the sodium nitrate–uranyl nitrate hexahydrate system. Hence, it is evident that the nature of the oxides in the calcined high-level waste reacting with glass forming additives during its conversion to glass form can be different from that considered by Mukerji and Kanyal. In view of this, it is essential to generate a database for the interactions among various nitrates of fission products and corrosion products of interest in the back end of the nuclear fuel cycle. The reaction between strontium nitrate and uranyl nitrate hexahydrate (UNH) at high temperatures has been studied using simultaneous TG-DTA-EGA and X-ray diffraction (XRD) techniques and the results are presented here.

---

[*] Corresponding author. Tel.: +91-22 25595096; fax: +91-22 25505151.

E-mail address: ravipv@apsara.barc.ernet.in (P.V. Ravindran).

0022-3115/03/$ - see front matter © 2003 Elsevier Science B.V. All rights reserved.
doi:10.1016/S0022-3115(03)00070-9

2. Experimental

TG-DTA-EGA measurements and XRD studies were carried out on the instruments described in an earlier communication [2]. The TG-DTA-EGA data were recorded simultaneously on the same sample in an argon flow maintained at 80 ml/min. Analytical reagent grade strontium nitrate (E. Merck AG, Germany) and UNH prepared [3] from nuclear grade uranium sesquioxide were used. Mixtures of UNH and strontium nitrate of the desired composition, containing 20, 30, 40, 50, 60, 70 or 80 mol% UNH, were gently ground to a uniform consistency and about 100 mg of the same weighed accurately was used in all measurements. Specimen holders made from recrystallised alumina were used and the heating rate was maintained at 10 K/min in all measurements. The temperatures for preparing the intermediate compounds/compositions for XRD measurements were determined from TG-DTA curves. All XRD measurements were carried out at room temperature on a Philips X-Ray Diffractometer, Model PW1710, using nickel-filtered Cu-Kα radiation. The intermediate compounds were prepared in situ in the thermal analyser in argon flow by heating at the selected heating rate to the desired temperature and cooling to room temperature by switching off the furnace power supply.

3. Results

Typical TG-DTA-EGA curves obtained for the mixtures of UNH and strontium nitrate are presented in Figs. 1 and 2. The data show absence of any direct reaction of UNH or its dehydration intermediates with strontium nitrate to form complex nitrates unlike in the case of mixtures of alkali metal nitrates and UNH [2]. In order to confirm this observation, XRD patterns were recorded (Fig. 3) for mixtures of the two nitrates heated in the thermobalance as in a normal TG-DTA experiment up to 560 °C – a temperature very close to but below the melting point of strontium nitrate (570 °C) [4] – and cooled to room temperature.

The TG-DTA-EGA curves above 560 °C for the various mixtures indicated reactions leading to the formation and decomposition of different nitrato-complexes of uranium and strontium depending on the composition of the mixture. This was further confirmed by checking for the presence of strontium nitrate as evidenced by the exotherm for the solidification of liquid strontium nitrate in mixtures heated up to 630 °C. Simultaneous TG-DTA curves in both heating and cooling modes were recorded (Fig. 4) in the temperature range of 25–630 °C for pure strontium nitrate as well as a mixture containing 50 mol% UNH, ensuring identical weight of strontium nitrate in the specimens for both measurements.

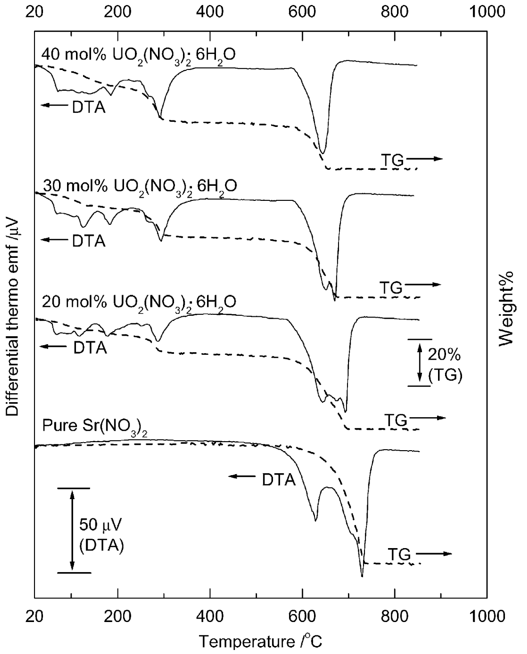

Fig. 1. TG-DTA curves for mixtures of UNH with strontium nitrate at a heating rate of 10 K min^{-1} in argon flow.

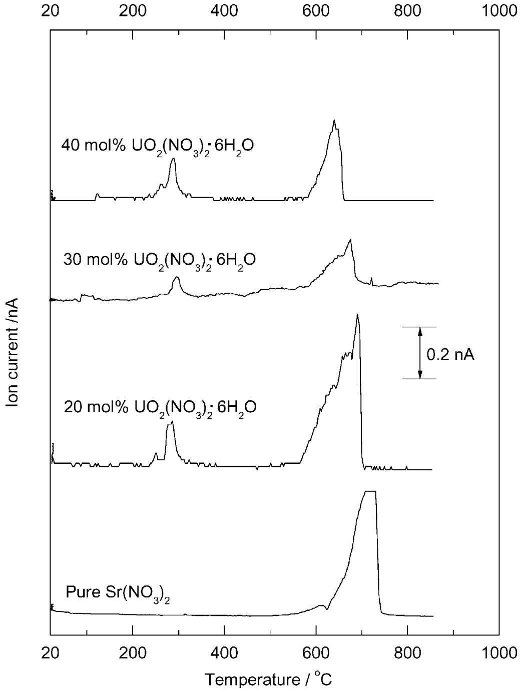

Fig. 2. EGA curves for the evolution of nitric oxide from mixtures of UNH and strontium nitrate at a heating rate of 10 K min^{-1} in argon flow.

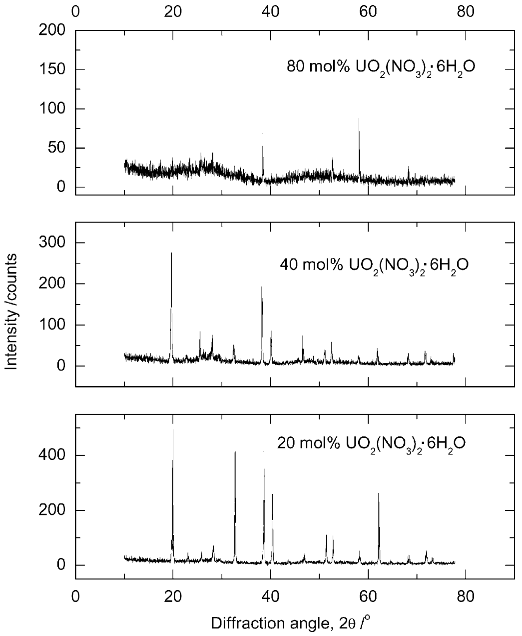

Fig. 3. XRD data for mixtures of UNH with strontium nitrate heated up to 560 °C.

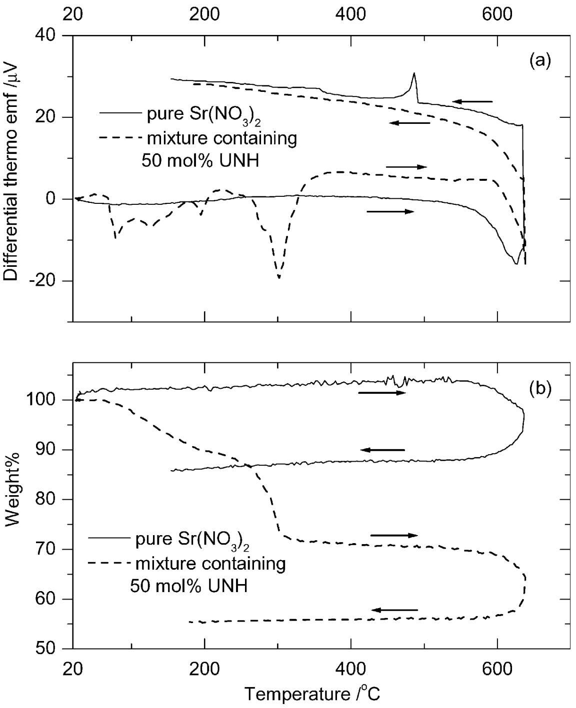

Fig. 4. (a) DTA and (b) TG curves for pure strontium nitrate and its mixture containing 50 mol% UNH in heating (——▶) and cooling (◀——) modes in argon flow at the heating/cooling rate of 10 K min^{-1}.

The intermediate compounds obtained at different temperatures above 600 °C were cooled to room temperature in situ in the thermal analyzer and analysed by XRD patterns. The results are presented in Figs. 5 and 6.

4. Discussion

4.1. Effect of strontium nitrate on hydrolysis and decomposition of uranyl nitrate hexahydrate

The first endothermic peak observed on the DTA curves (Fig. 1) for the mixtures of UNH and strontium nitrate is due to melting of the partially dehydrated UNH [3]. The corresponding peak temperature of 70 °C is in conformity with earlier results for pure UNH from our laboratory [3]. Lodding and Ojamaa [5] reported a DTA peak temperature of 65 °C for melting in UNH as against a value of 60.2 °C reported from melting point determination [4,6]. The difference between these results is not significant considering the effects of heating rate and other experimental variables on DTA curves. The equilibrium temperature is considered closer to the

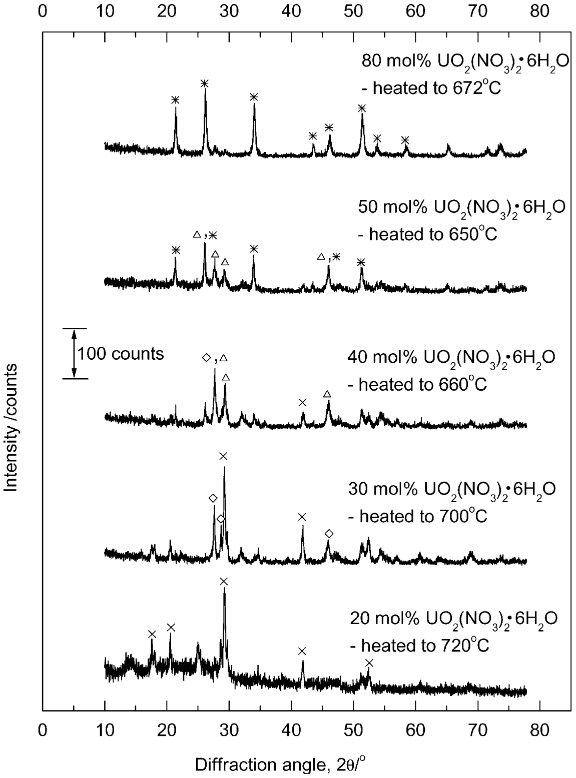

Fig. 5. XRD data for the final products of high temperature reactions in various mixtures of UNH and strontium nitrate. △ – $SrUO_4$, ∗ – SrU_4O_{13}, M – Sr_2UO_5, ◇ – Sr_3UO_6.

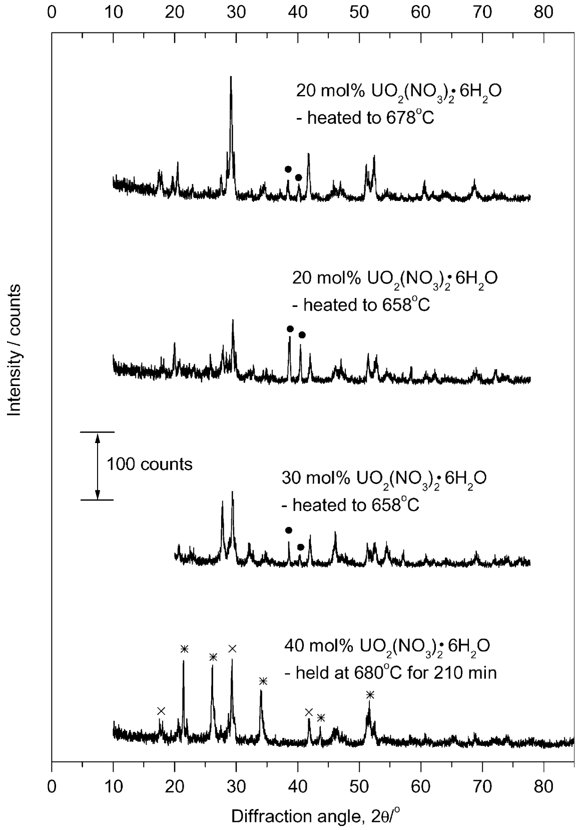

Fig. 6. XRD data for the reaction intermediates formed above 565 °C from mixtures of UNH and strontium nitrate. • – Complex I, Complex II, ∗ – SrU_4O_{13}, ◇ – Sr_3UO_6.

extrapolated on-set temperature read from DTA curves rather than the peak temperature [7]. However, because of an overlap of the melting in UNH with dehydration of the salt, the extrapolated on-set temperature for the melting endotherm cannot be determined in the present case.

The susceptibility of UNH to hydrolysis in the water of crystallization released on heating [8,9] has led to much variability in the pattern of dehydration at atmospheric pressure observed by various authors [10]. While early work [5,11] suggested dehydration of UNH in successive steps to form trihydrate, dihydrate, monohydrate and the anhydrous salt, other workers [3,12] have shown that hydroxynitrates of uranium, rather than well-defined hydrates are formed during the dehydration process. It is now an accepted fact [13] that anhydrous uranyl nitrate cannot be obtained by the thermal decomposition of UNH because of hydrolysis of the salt in the water vapour evolved during dehydration. Our earlier results [3] from EGA measurements showed an overlap of evolution of water vapour and oxides of nitrogen during the decomposition of UNH in the temperature range of 225–400 °C. The evolution of oxides of nitrogen occurred in multiple step up to 550 °C. Furthermore, the intensity of the corresponding higher temperature peaks increased at the expense of the lower temperature peaks with increase in heating rate and sample size. These observations were interpreted as indicative of hydrolysis of uranyl nitrate and polymerisation of the resulting hydroxynitrates in presence of the accumulated water vapour around the dehydrated reactant particles. Such hydrolysis and polymerisation are not significant when UNH is decomposed in presence of strontium nitrate as evidenced by the total absence of the EGA peaks for the evolution of nitric oxide in the temperature range of 375–550 °C (Fig. 2). Hence, the weight loss up to 220 °C as observed from TG data (Fig. 1) recorded simultaneously with DTA for mixtures of UNH and strontium nitrate, corresponds to the formation of $UO_2(NO_3)_2 \cdot 2H_2O$ rather than a hydroxynitrate of uranium (Table 1) and the overall reaction in the temperature interval of 40–220 °C could be represented by the equation:

$$UO_2(NO_3)_2 \cdot 6H_2O \xrightarrow[Sr(NO_3)_2]{40\text{–}220\ ^\circ C} UO_2(NO_3)_2 \cdot 2H_2O + 4H_2O \tag{1}$$

The DTA and EGA peaks for the evolution of nitric oxide in the temperature range 225–375 °C and the corresponding weight loss step on the TG curve are due to the decomposition of uranyl nitrate dihydrate to amorphous UO_3. The XRD patterns (Fig. 3) for the residue obtained at 560 °C for different compositions of the mixture of the two nitrates show the presence of amorphous UO_3 [2,12] along with strontium nitrate [14]. Amorphous UO_3 predominates for compositions rich in UNH. These results point to the fact that strontium nitrate, unlike in the case of sodium nitrate [2], does not form any complex nitrate directly with UNH. Hence, UNH in the mixture decomposes as an independent entity forming amorphous UO_3.

$$UO_2(NO_3)_2 \cdot 2H_2O \xrightarrow[Sr(NO_3)_2]{225\ ^\circ C} UO_3 + NO_2 + NO + O_2 + 2H_2O \tag{2}$$

4.2. Interaction between uranium trioxide and strontium nitrate

The TG-DTA curves presented in Fig. 4 show that pure strontium nitrate starts to decompose above 560 °C as evident from the weight change indicated by the TG curve above this temperature. Simultaneously, it melts and the two processes are observed as two overlapping endothermic peaks in Fig. 1. Since the extent of decomposition during the melting process is not significant, the

Table 1
Thermogravimetric data for phase compositions in mixtures of uranyl nitrate and strontium nitrate

Composition of the mixture (mol% UNH)	Temperature range (°C)	Weight loss % observed[a]	Weight loss % calculated[a]	Reaction
20	40–215	5.5	5.34	$UO_2(NO_3)_2 \cdot 6H_2O \rightarrow UO_2(NO_3)_2 \cdot 2H_2O + 4H_2O$
	225–560	10.0	10.68	$UO_2(NO_3)_2 \cdot 2H_2O \rightarrow UO_3 + NO_2 + NO + O_2 + 2H_2O$
	560–710	31.0	32.04	$UO_3 + 4Sr(NO_3)_2 \rightarrow Sr_3UO_6 + SrO + 8NO + 6O_2$
30	40–210	7.3	7.23	$UO_2(NO_3)_2 \cdot 6H_2O \rightarrow UO_2(NO_3)_2 \cdot 2H_2O + 4H_2O$
	225–560	13.3	14.46	$UO_2(NO_3)_2 \cdot 2H_2O \rightarrow UO_3 + NO_2 + NO + O_2 + 2H_2O$
	560–680	24.0	25.31	$3UO_3 + 7Sr(NO_3)_2 \rightarrow 2Sr_2UO_5 + Sr_3UO_6 + 14NO + \frac{21}{2}O_2$
40	40–210	9.0	8.79	$UO_2(NO_3)_2 \cdot 6H_2O \rightarrow UO_2(NO_3)_2 \cdot 2H_2O + 4H_2O$
	225–560	16.8	17.57	$UO_2(NO_3)_2 \cdot 2H_2O \rightarrow UO_3 + NO_2 + NO + O_2 + 2H_2O$
	565–660	18.8	17.77	$2UO_3 + 3Sr(NO_3)_2 \rightarrow SrUO_4 + Sr_2UO_5 + 6NO + \frac{9}{2}O_2$
50	45–210	9.5	10.09	$UO_2(NO_3)_2 \cdot 6H_2O \rightarrow UO_2(NO_3)_2 \cdot 2H_2O + 4H_2O$
	225–560	20.0	20.18	$UO_2(NO_3)_2 \cdot 2H_2O \rightarrow UO_3 + NO_2 + NO + O_2 + 2H_2O$
	565–660	14.0	15.13	$UO_3 + Sr(NO_3)_2 \rightarrow SrUO_4 + 2NO + \frac{3}{2}O_2$
80	40–210	12.3	12.98	$UO_2(NO_3)_2 \cdot 6H_2O \rightarrow UO_2(NO_3)_2 \cdot 2H_2O + 4H_2O$
	220–560	24.5	25.95	$UO_2(NO_3)_2 \cdot 2H_2O \rightarrow UO_3 + NO_2 + NO + O_2 + 2H_2O$
	565–645	5.3	4.87	$4UO_3 + Sr(NO_3)_2 \rightarrow SrU_4O_{13} + 2NO + \frac{3}{2}O_2$

[a] Based on the initial weight of the mixture of UNH and strontium nitrate.

melting point can be obtained as the extrapolated on-set temperature of the first endotherm, which is shown also in the heating curve of Fig. 4(a). The melting point so obtained from Fig. 4(a) is 580 °C, which is in good agreement with the reported value considering that the DTA signal observed for melting is also influenced by partial decomposition of strontium nitrate. The fusion exotherm is observed in the cooling mode with an extrapolated on-set temperature of 490 °C. The decrease in magnitude and temperature of the fusion exotherm compared to the melting endotherm is possibly because of the partial decomposition of strontium nitrate during melting. In the case of the 50 mol% mixture (Fig. 4(b)), no heat effect was detected in the cooling mode in spite of the weight of strontium nitrate in the mixture being equal to that used for the experiment with the pure component. This proved absence of strontium nitrate in the mixture heated to temperatures greater than or equal to 630 °C, the maximum temperature attained in the heat–cool cycle. However, the temperatures of maxima on profiles for evolution of nitric oxide (Fig. 2) in the temperature range of 565–800 °C are $\geqslant 640$ °C. This higher temperature evolution of nitric oxide can result from a newly formed nitrato-complex. Hence, it is evident that strontium nitrate in the mixture reacts with UO_3 as soon as it melts to form a complex nitrate of uranium and strontium.

The TG and DTA curves above 565 °C (Fig. 1) show a variability depending on the composition of the initial nitrate mixture. The number of DTA peaks for the overall reaction leading to the formation of a stable uranate phase and the temperature span of the overall reaction increase with decreasing amount of UNH in the initial nitrate mixture. This is indicative of a change in mechanism of the reaction with composition of the mixture. The patterns for the evolution of nitric oxide above 565 °C (Fig. 2) confirm that the multiple heat effects observed on the DTA curve correspond to the formation and decomposition of various nitrato-complexes. A comparison with the decomposition pattern for pure strontium nitrate also indicates that the evolution of nitric oxide for pure strontium nitrate occurs over a wider temperature interval than for its mixtures with UNH. The XRD patterns presented in Fig. 5 for the final residues from TG-DTA-EGA measurements show the evolution of various uranate phases dependent on the initial composition of the nitrate mixture.

4.2.1. Compositions containing 40 mol% or more uranyl nitrate hexahydrate

For compositions containing 40 mol% or more UNH, the formation of the uranate was completed by 660 °C. The corresponding DTA curve (Fig. 1) scanned up to the temperature of 715 °C shows only a single endothermic peak ending at about 660 °C. In the case of a mixture containing 80 mol% UNH, the XRD pattern (Fig. 5) for the residue obtained at 672 °C corresponds predominantly to that for SrU_4O_{13} [15,16]. The weight loss read from the corresponding TG curve is in good agreement with the theoretical value (Table 1) calculated based on the equation:

$$4UO_3 + Sr(NO_3)_2 \xrightarrow{565\ ^\circ C} SrU_4O_{13} + 2NO + \tfrac{3}{2}\,O_2 \qquad (3)$$

On decreasing the UNH content of the mixture to 50 mol%, the diffraction peaks at the 2θ values of 21.5°, 26.3° and 34° decrease in intensity (Fig. 5) and the XRD pattern for the final residue shows presence of α-$SrUO_4$ [17]. The weight loss data in the temperature range 565–650 °C for the mixture correspond, within experimental errors, to the reaction given by

$$UO_3 + Sr(NO_3)_2 \xrightarrow{565\ ^\circ C} SrUO_4 + 2NO + \tfrac{3}{2}\,O_2 \qquad (4)$$

It is possible that part of the UO_3 available may react with $SrUO_4$ thus formed to give SrU_4O_{13}. Hence, the XRD pattern also shows presence of SrU_4O_{13} along with $SrUO_4$.

When the UNH content in the initial nitrate mixture is further reduced to 40 mol% level, XRD of residues obtained at 660 °C shows an increase in intensity of diffraction peaks at 27.5° and 29.3° at the expense of the peak at 26.3°. The pattern (Fig. 5) corresponds to a mixture of α-$SrUO_4$ and Sr_2UO_5 [18]. The weight loss observed from the TG curve in the temperature interval 565–660 °C is in agreement with the reaction stoichiometry represented by the equation:

$$2UO_3 + 3Sr(NO_3)_2 \xrightarrow{565\ ^\circ C} SrUO_4 + Sr_2UO_5 + 6NO + \tfrac{9}{2}\,O_2 \qquad (5)$$

4.2.2. Compositions containing less than 40 mol% uranyl nitrate hexahydrate

The mixture containing 30 mol% UNH decomposes above 565 °C in two endothermic steps accompanied by the evolution of nitric oxide (Fig. 2). Apparently, a stable intermediate nitrato-complex is formed as a result of the reaction between UO_3 and strontium nitrate in the mixture, and the first peak on the DTA curve (Fig. 1) in the temperature interval of 565–660 °C corresponds to the formation reaction. The second peak observed between 660 and 680 °C is due to the decomposition of the intermediate to uranate. The formation of uranate is completed only by 680 °C in the present set of experiments. The intermediate prepared by heating the mixture to 658 °C (valley between the two DTA peaks) and cooling the residue to room temperature showed two additional peaks at 2θ values of 38.5° and 40.3° in the XRD pattern (Fig. 6). These peaks disappear on heating the mixture to 700 °C (Fig. 5) leaving a residue of the uranate, Sr_2UO_5. Although peaks at the corresponding diffraction angles are also seen in the XRD pattern of pure strontium nitrate (Fig. 3), the most intense peak for strontium nitrate at the 2θ value of 19.74°, is not prominent in Fig. 6. Hence, the peaks at 2θ values of 38.5° and 40.3° cannot be ascribed to excess undecomposed strontium nitrate in the mixture. Furthermore, the data presented in Fig. 4 confirm absence of strontium nitrate in its mixtures with UNH at the temperature of 630 °C and above. It is therefore evident that the two new peaks at 38.5° and 40.3° in the XRD pattern of the residue obtained at 660 ° C in Fig. 6 are characteristic of a new complex nitrate of uranium and strontium. Since this complex decomposes to Sr_2UO_5 (Fig. 5) having an Sr/U ratio of 2, it is only natural to expect an identical Sr/U ratio in the complex nitrate. Its structural formula may therefore be represented as

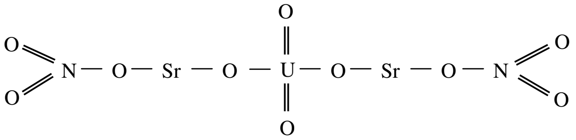

Complex I

and its formation by reaction of UO_3 with strontium nitrate may be given by Eq. (6)

$$UO_3 + 2Sr(NO_3)_2 \xrightarrow{565\ ^\circ C} (UO_2)(OSrNO_3)_2 + 2NO + \tfrac{3}{2}\,O_2 \qquad (6)$$

This complex decomposes evolving nitric oxide above 660 ° C to form the uranate, Sr_2UO_5, as shown in Eq. (7).

$$(UO_2)(OSrNO_3)_2 \xrightarrow{660\ ^\circ C} Sr_2UO_5 + 2NO + \tfrac{3}{2}\,O_2 \qquad (7)$$

The 30 mol% UNH mixture employed in this study is slightly richer in strontium nitrate concentration compared to that represented by Eq. (6). It is possible that the excess amount of strontium nitrate decomposes to give strontium oxide, which further reacts with Sr_2UO_5 to form Sr_3UO_6 as indicated in Table 1. The weight loss observed from TG data is slightly lower than that calculated by the equation suggested in Table 1. However, peaks for Sr_3UO_6 are present in XRD patterns (Fig. 5) for all compositions rich in strontium nitrate.

The decomposition of the mixture containing 20 mol% UNH is completed only by 715 °C. The corresponding DTA curve (Fig. 1) showed a triplet endotherm also accompanied by the evolution of nitric oxide in the temperature range of 565–715 °C (Fig. 2). This indicates the formation and decomposition of two intermediate nitrato-complexes differing in thermal stability. The first DTA peak observed in the temperature range of 565–660 °C (Fig. 1) corresponds to the formation of these nitrato-complexes. The XRD patterns for residues prepared at 658 and 678 °C (Fig. 6) from this mixture also showed the peaks at 2θ values of 38.5° and 40.3°. The intensities for both the peaks are lower for the residue prepared at 678 °C as compared to that obtained at 658 °C. This shows that both the intermediate complexes contribute to the intensities of the two peaks and that one of the complexes is unstable above 658 °C. These peaks disappear on heating the mixture to higher temperatures (Fig. 5) leaving behind a residue of Sr_3UO_6 [18]. The DTA peak in the temperature range of 660–680 °C (Fig. 1) corresponds to the decomposition of the less stable complex and the endotherm in the temperature interval 680–715 °C corresponds to the decomposition of the more stable complex. Since the XRD patterns for the residues prepared at 658 and 678 °C from this mixture are similar to that for the residue prepared at 658 °C from the mixture containing 30 mol% UNH (Fig. 6), it is apparent that the three complexes are similar in structure. The DTA and EGA peaks in the temperature range of 660–680 °C in Figs. 1 and 2 for the two compositions are also at identical temperatures. It is therefore concluded that the complex decomposing in the temperature range of 660–680 °C and formed from the mixture containing 20 mol% UNH is the same as Complex I discussed above. The other complex (II) is stable up to 680 °C because of a higher ratio of Sr/U in its molecule and its structural formula may be represented as

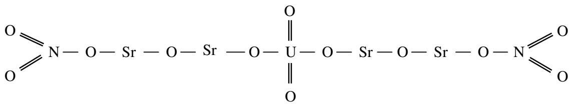

Complex II

The thermoanalytical and XRD data presented here suggest that both the complexes are present at 660 °C in the case of mixture containing 20 mol% UNH. These may be formed at temperatures above 565 °C according to Eq. (8).

$$2UO_3 + 8Sr(NO_3)_2 \xrightarrow{565\ ^\circ C} (UO_2)(OSrNO_3)_2 + (UO_2)(OSr)_2(OSrNO_3)_2 + 2SrO + 12NO + 9O_2 \tag{8}$$

At temperatures above 680 °C Complex II reacts with the uranate, Sr_2UO_5 formed by the decomposition of Complex I (Eq. (7)) to form Sr_3UO_6 [18] in accordance with Eq. (9),

$$(UO_2)(OSr)_2(OSrNO_3)_2 + Sr_2UO_5 \xrightarrow{680\ ^\circ C} 2Sr_3UO_6 + 2NO + \tfrac{3}{2}O_2 \tag{9}$$

The weight losses observed (Table 1) for various mixtures are in fairly good agreement with the theoretical values calculated from Eqs. (1)–(9). The presence of SrO could not be observed from the XRD patterns presented in Figs. 5 and 6 as the amount formed is relatively small and the peaks for SrO overlap partially with those for Sr_3UO_6.

In view of the heterogeneous nature of the solid state reactions, the reactions represented by Eqs. (3)–(9) may occur simultaneously, although to various extents depending on the locally available composition and temperature of the mixture, intimacy of contact between the reactant particles, etc. In addition, uranium trioxide and strontium oxide, formed by a partial decomposition of strontium nitrate, will further react with the uranates derived from a specific composition to form uranium rich or strontium rich uranates. Hence, the products obtained by thermoanalytical experiments are not expected to have phase purity and this is reflected in the XRD patterns presented in Figs. 5 and 6. Efforts to obtain phase pure uranate by maintaining the final residue at high temperature for longer times (Fig. 6) result in the disproportionation of the uranates.

5. Conclusions

The present studies indicate that strontium nitrate does not react directly with UNH, although it affects the extent of hydrolysis and polymerisation of the latter during its dehydration and decomposition. The amorphous uranium trioxide formed as a result of the decomposition of UNH, however, reacts with strontium nitrate immediately after the latter compound melts and forms complex nitrates of uranium and strontium. The stoichiometry of these complex nitrates varies with the composition of the initial nitrate mixture as evidenced by their decomposition patterns. The complex nitrates so formed show an increase in thermal stability with an increase in Sr/U ratio. These decompose to give various uranates of strontium, depending on the stoichiometry of the complex. The complex formation ensured that the conversion of nitrate to oxide is completed at temperatures lower than that for pure strontium nitrate.

References

[1] J. Mukerji, P.B. Kanyal, Bhabha Atomic Research Centre Report, BARC-691, 1973.
[2] B.B. Kalekar, K.V. Rajagopalan, C.G.S. Pillai, P.V. Ravindran, P.K. Mathur, J. Nucl. Mater. 279 (2000) 245.
[3] K.V. Rajagopalan, P.V. Ravindran, T.P. Radhakrishnan, J. Therm. Anal. 44 (1995) 89.
[4] J.A. Dean (Ed.), Lange's Handbook of Chemistry, 14th Ed., McGraw-Hill, Inc, New York, 1992, p. 3-56.
[5] W. Lodding, L. Ojamaa, J. Inorg. Nucl. Chem. 27 (1965) 1261.
[6] D.R. Linde, H.P.R. Frederikse, Handbook of Chemistry and Physics, 76th Ed., CRC, Boca Raton, 1995, p. 4-94.

[7] R.C. Mackenzie, C.J. Keattch, D. Dollimore, J.A. Forrester, A.A. Hodgson, J.P. Redfern, Thermochim. Acta 5 (1972) 71.
[8] J.L. Woodhead, A.M. Dean, A.C. Fox, J.M. Fletcher, J. Inorg. Nucl. Chem. 28 (1966) 2175.
[9] M. Åberg, Acta Chem. Scand., Ser. A 32 (1978) 101.
[10] R. Becker, H. Holleck, H. Kleykamp, L. Stieglitz, in: R. Keim (Ed.), Gmelin Handbook of Inorganic Chemistry, Uranium, Supplement, Vol. C7, Springer-Verlag, Berlin, 1981, p. 140.
[11] W.H. Smith, J. Inorg. Nucl. Chem. 30 (1968) 1761.
[12] R.S. Ondrejcin, T.P. Garrett Jr., J. Phys. Chem. 65 (1961) 470.
[13] F. Weigel, in: J.J. Katz, G.T. Seaborg, L.R. Morss (Eds.), The Chemistry of Actinides, 2nd Ed., Vol. 1, Chapmann and Hall, London, 1986, p. 361.
[14] JCPDS International Centre for Diffraction Data, Powder Diffraction File, Card no. 25-0746.
[15] E.H.P. Cordfunke, B.O. Loopstra, J. Inorg. Nucl. Chem. 29 (1967) 51.
[16] E.H.P. Cordfunke, P. van Vlaanderen, M. Onink, D.J.W. Ijdo, J. Solid State Chem. 94 (1991) 12.
[17] W.H. Zachariasen, Acta Crystallogr. 1 (1948) 281.
[18] JCPDS International Centre for Diffraction Data, Powder Diffraction File, Card no. 73-0771; 73-0773.